CARBON 72 (2014) 304–311

Available at www.sciencedirect.com

ScienceDirect

journal homepage: www.elsevier.com/locate/carbon

Improvement of stacking order in graphite by molten fluoride salt infiltration

He Zhoutong [a,*], Gao Lina [a], Wang Xue [a], Zhang Baoliang [a,c], Qi Wei [a,b], Song Jinliang [a], He Xiujie [a,c], Zhang Can [a], Tang Hui [a], Xia Huihao [a,*], Zhou Xingtai [a,*]

[a] Key Laboratory of Nuclear Radiation and Nuclear Energy Technology, Chinese Academy of Sciences, Shanghai 201800, PR China
[b] University of Chinese Academy of Sciences, Beijing 100049, PR China
[c] School of Physics, Shandong University, Jinan 250100, PR China

ARTICLE INFO

Article history:
Received 14 October 2013
Accepted 1 February 2014
Available online 10 February 2014

ABSTRACT

The structure of molten fluoride salt infiltrated graphite has been studied by X-ray diffraction and Raman spectroscopy. The full width at half maximum and asymmetry degree of the (002) diffraction peak decrease with the increase of salt weight gain in the infiltration indicates the improvement of the stacking order of the graphite by the molten salt infiltration. The shape of G′ resonance of Raman spectra further indicated the enhancement of the stacking order of graphite by molten salt infiltration. The shift of the (002) diffraction peak position to the higher 2θ angle and the increase of the coefficient of thermal expansion reveal that the improvement of the stacking order is resulted from the compression of the graphite matrix by the infiltrated salt network. The compressive stress induced by the salt network in the graphite matrix could reduce the d-spacing fluctuation between graphite basal planes and close the Mrozowski crack generated by the anisotropy of graphite crystal, thus increase the crystallite size along *c*-axis.

1. Introduction

Artificial graphite is a very versatile material. It is used in a wide range of applications and extreme environments. For example: it is immersed in molten salts while used as electrode in electrolytic process for production of aluminum and rare earth metal [1–3], due to its inert chemistry properties and good electrical properties; it is also used as moderator and reflector in molten salt reactor for its high moderating ratio and good irradiation resistance [4–6]. But due to its porous nature, molten salts may infiltrate the graphite [7]. In other cases, metals, such as copper, silver, aluminum and lead etc., are infiltrated into graphite in order to obtain composites with low thermal expansion combined with relatively high mechanical strength or high electrical conductivity [8,9]; glasses are infiltrated into graphite to prepare packaging materials with high thermal conductivity [10]; molten salts are infiltrated into graphite to produce reliable phase change material for energy storage [11,12] and gas impermeable graphite for molten salt reactor graphite core [13]. However, the structure evolution of the graphite during the infiltration process is not clear.

Artificial graphite is poly-granular with an average pore size range from several hundreds of nanometers to several tens of micrometers which varies depending on the raw material used and the production process [14,15]. Because of the weak van der Waals force between the basal planes of graphite crystal and the large difference between the

---

* *Corresponding authors*: Fax: +86 21 39194539.
E-mail addresses: hezhoutong@sinap.ac.cn (Z. He), xiahuihao@sinap.ac.cn (H. Xia), zhouxingtai@sinap.ac.cn (X. Zhou).

http://dx.doi.org/10.1016/j.carbon.2014.02.010

coefficient of thermal expansion (CTE) along *c*-axis and *a*-axis of graphite crystal, graphite is inherent with d-spacing fluctuation and micro-cracks which are also called Mrozowski cracks [16,17]. The d-spacing fluctuation and the Mrozowski cracks are very important to the utility of the graphite. They accommodate the expansion of graphite crystal along *c*-axis at elevated temperature [18–20] and the early stage of irradiation [16,17,21].

The infiltrated phase in graphite, such as metal, glass or molten salt could induce stress in the graphite while cooling down to room temperature due to the mismatch in the CTE between the infiltrated phase and graphite matrix [8,10,22]. The stress may affect the d-spacing fluctuation and the Mrozowski cracks in graphite, thus influence the properties of graphite used in extreme conditions, for example as a moderator and reflector in molten salt reactor [16]. Though the increase of crystallinity degree of graphite in molten salt was reported by Kamali et al. [23,24], where the corrosion plays an important role, there is no reported research about the impact of molten salt induced stress on graphite structure to the authors' best knowledge.

d-Spacing fluctuation and Mrozowski cracks can be observed by X-ray diffraction (XRD) [16,25] and Raman spectroscopy [26], as they break the stacking order of graphite basal plane. The reduction in the d-spacing fluctuation and closure of Mrozowski cracks enhance the crystalline order of graphite along *c*-axis and would be expected to reduce the full width at half maximum (FWHM) of the (002) diffraction peak. The improvement of stacking order in graphite may be observed by the shape of G′ resonance peak of Raman spectra [27,28].

In this work, six grades of graphite were infiltrated by molten fluoride salt under different pressures in order to obtain infiltrated graphite samples with different weight gains. XRD was used to determine the structure changes of the samples. The changes in shape and FWHM of the graphite (002) diffraction peak in XRD spectra were used to compare the stacking order of the graphite with different weight gains due to infiltration. And shape of G′ resonance in the Raman spectra was also used as evidence of the enhancement of the stacking order due to molten salt infiltration. The mechanism of the stacking order improvement was discussed in relation to stress evolution which was evidenced by the position shift and shape change of the graphite (002) diffraction peak and the CTE change after molten salt infiltration.

2. Experimental

The graphite samples used in the experiment were 2020 and 2114 from Mersen, IG-110 from Toyo Tanso, NBG-18 from SGL Carbon group and two under developing graphite grades from China referred as G1 and G2. The raw material used and the properties of these grades of graphite are shown in Table 1 [29]. The graphite samples were machined to Ø12.7 × 38.1 mm in dimension and marked by a laser marking machine, and then cleaned with ethyl alcohol followed with vacuum drying for 2 h at a temperature of 150 °C. After weighing, graphite samples were infiltrated with about 0.5 liter molten salt in a pressure vessel at 650 °C for 20 h. The molten salt used was the eutectic salt of LiF, NaF and KF (FLiNaK, LiF–NaF–KF: 46.5–11.5–42 mol%), which has a melting point of about 450 °C. The graphite samples were evacuated before immersing in the molten salt. The infiltration pressure used was varied from 1 to 10 atm, which was controlled by the pressure of the argon cover gas. The graphite samples were pulled out from the molten salt after 20 h of infiltration. The pressure in the pressure vessel was maintained until the pressure vessel had cooled to room temperature. In order to avoid the oxidation of graphite in high temperature, the total oxygen content in the molten salt is less than 200 ppm and the purity of argon used is 99.999%. For the unwetting nature of the molten salt with graphite, there was only a small quantity of FLiNaK salt attached on the graphite sample surface after infiltration, which could be removed by scratching. The graphite samples was cleaned and weighted in an oxygen- and water-free glove box to determine the weight gain of the graphite samples in the infiltration process.

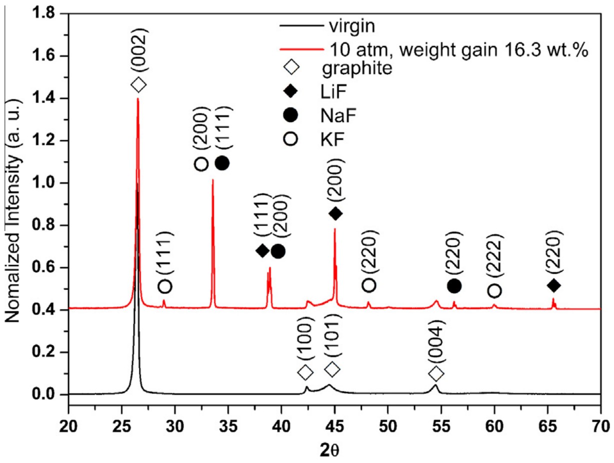

Fig. 1 – The XRD spectra of virgin IG-110 (black line) and 10 atm molten salt infiltrated IG-110 (red line). The corresponding Miller index of each peak is as labeled. (A color version of this figure can be viewed online.)

Table 1 – The description and properties of the graphite samples.

Grade	Coke type	Grain size	Forming way	Bulk density
2020	Pet	15 μm	Isostatic-molded	1.77 g/cm^3
2114	Non-pet	13 μm	Isostatic-molded	1.81 g/cm^3
IG-110	Pet	20 μm	Isostatic-molded	1.77 g/cm^3
NBG-18	Pitch	1.6 mm maximum	Vibration-molded	1.86 g/cm^3
G1	Pitch	10 μm	Isostatic-molded	1.82 g/cm^3
G2	Natural graphite	20 μm	Isostatic-molded	~1.72 g/cm^3